Magnetic properties and interactions in the $R\mathrm{Mn}_{12-x}\mathrm{Fe}_x$ series ($R=$ Y, Ho, Er, Nd; $x\leqslant9$)

M. Morales,[1,2,*] M. Bacmann,[1] P. Wolfers,[1] D. Fruchart,[1] and B. Ouladdiaf[3]

[1]*Laboratoire de Cristallographie du CNRS, BP166, 38042 Grenoble Cedex 09, France*
[2]*Instituto de Ciencias de Materiales de Aragon, Ciudad Universitaria 50009, Zaragoza, Spain*
[3]*Institut Laue Langevin, 6 rue Jules Horowitz, 38042 Grenoble Cedex 09, France*

Powder neutron thermodiffraction studies have allowed a precise determination of the magnetic phase diagrams of the $R\mathrm{Mn}_{12-x}\mathrm{Fe}_x$ series (ThMn$_{12}$ structure) with the occurrence of two different ordering temperatures T_N and T_C correlated, respectively, to antiferromagnetic and ferromagnetic couplings. At low iron contents ($x\leqslant5$) and for all R elements, the $3d$ metal sublattices exhibit antiferromagnetic (AF) configurations lying in the basal plane (a, b). The R magnetic moments order ferromagnetically at very low temperature only with c as an easy axis. For higher iron concentrations, the $3d$ magnetic moment arrangements change progressively with ferromagnetic (F) components collinear with the c axis superimposed on the AF components. For $x>6$, the Curie temperature T_C coming from the F components of the $3d$ and R sublattices increases markedly. In addition, T_N and the $3d$ AF components both decrease with x.

I. INTRODUCTION

During the past few decades, considerable attention has been paid to the study of intermetallic compounds of rare-earth elements (R) and $3d$ magnetic transition metals (M).[1] The compounds with nominal composition $R\mathrm{Fe}_{12}$, having the ThMn$_{12}$ structure,[2] do not exist, but can be stabilized by partial substitution of iron by a metal M with a lower valence electron density.[3] In contrast to the mostly ferromagnetic (F) character of the iron-rich compounds, the parent $R\mathrm{Mn}_{12}$ ones exhibit antiferromagnetic (AF) ordering at low temperature.[4] Consequently, complex magnetic behaviors are expected to occur in the $R\mathrm{Mn}_{12-x}\mathrm{Fe}_x$ solid solutions as a result of the competing F and AF interactions. In order to get a representative sample group of compounds, different R elements were selected, such as the nonmagnetic yttrium, the heavy rare-earth elements holmium (second-order Stevens factor $\alpha_J<0$) and erbium ($\alpha_J>0$), and finally the light rare-earth element neodymium ($\alpha_J<0$). In the present paper, the R-$3d$ and $3d$-$3d$ magnetic interactions are studied as a function of the iron concentration x(Fe) and temperature using neutron diffraction measurements. Previous macroscopic magnetic studies on the $R\mathrm{Mn}_{12-x}\mathrm{Fe}_x$ compounds have permitted the observation of different magnetic behaviors depending on the Fe content.[5] On the one hand, with the magnetic rare earths $R=$ Er, Ho, and Nd for $x<6$, two ordering temperatures T_N and T_C were observed corresponding, respectively, to AF and F ordering. For the nonmagnetic element, $R=$ Y with $x<8$, only the AF ordering is observed for temperatures $T\leqslant T_N$. On the other hand, for the iron-rich compounds ($R=$ Nd, Ho, and Er and $6\leqslant x\leqslant8$; $R=$ Y and $x=8$), these two ordering temperatures are still observed, but the F ordering temperatures T_C are higher than those observed for the manganese-rich compounds. Finally, the iron-rich compounds ($x=9$ with $R=$ Er and Ho) exhibit only ferromagnetic behavior (only T_C is observed).

II. EXPERIMENT

The samples were produced in the concentration range $0\leqslant x\leqslant9$ by induction melting of the different constituents (99.9% purity) in a water-cooled copper crucible under a pressure of 1.2 bar of purified argon. The purity of the resulting phase was checked using x-ray powder diffraction. In some cases, small amounts of β-manganese and $R_6(\mathrm{Mn},\mathrm{Fe})_{23}$ were detected in the compounds belonging to the manganese-rich compounds ($x\leqslant4$). The $R_2\mathrm{Fe}_{17}$ impurity was identified in the compounds with $x=9$. The crystal structure of these compounds was determined using the high-resolution diffractometer D2B ($\lambda=1.594\,\text{Å}$) at the ILL (Grenoble, France). All the diffraction patterns were recorded at room temperature, where only nuclear scattering was observed. Rietveld refinements were carried out using the FULLPROF program,[6] assuming that each $3d$ metal site is fully occupied by iron and manganese atoms.[7] The magnetic configurations of the $R\mathrm{Mn}_{12-x}\mathrm{Fe}_x$ series were determined using neutron powder diffraction experiments with the D1B ($\lambda=2.522\,\text{Å}$) and D20 ($\lambda=2.40\,\text{Å}$) diffractometers, in the temperature range 2–300 K. The magnetic structure refinements were performed using the MXD program.[8]

III. STRUCTURAL PROPERTIES

All the samples were found to crystallize in the ThMn$_{12}$ structure type of space group $I4/mmm$ with 2 formula units.[2] The R atoms occupy the $2a$ site, whereas the $3d$(Mn, Fe) atoms occupy the three sites $8i$, $8j$, and $8f$ (Fig. 1). The
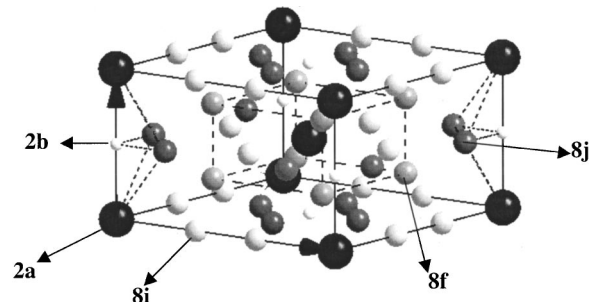
FIG. 1. Tetragonal crystal structure of the ThMn$_{12}$ type.

large contrast in the nuclear scattering lengths of iron and manganese permits an accurate determination of the $3d$ site occupations as a function of x and R. In Fig. 2, the iron occupation for each $R\mathrm{Mn}_{12-x}\mathrm{Fe}_x$ compound is compared with the occupation expected in the case of a random distribution represented by the diagonal line. For all R, iron atoms preferentially occupy the $8f$ sites, whereas manganese atoms are found preferentially on the $8i$ sites. It is clearly evidenced that the $3d$ metal occupation is independent of the nature of the rare-earth element.

In the $R\mathrm{Mn}_{12-x}\mathrm{Fe}_x$ compounds, for a fixed iron concentration, the a and c cell parameters decrease from $R=\mathrm{Nd}$ to Er in agreement with the lanthanide contraction. For a given rare-earth element R, the a cell parameter decreases linearly with the iron concentration, whereas the c cell parameter remains almost constant, resulting in a unit-cell volume decrease with a mean slope of 1.1 Å^3/Fe.[7]

IV. MAGNETIC PROPERTIES

Preliminary magnetization measurements have shown that the magnetic properties of the $R\mathrm{Mn}_{12-x}\mathrm{Fe}_x$ compounds are markedly dependent on the nature of the $3d(\mathrm{Mn},\mathrm{Fe})$ sublattices, which order antiferromagnetically for the manganese-rich compounds and ferromagnetically for the iron-rich compounds.[5]

For all $x<9$ and all R, no magnetic contributions are observed at room temperature in the neutron diffraction patterns. At low temperature ($T\lesssim 20\,\mathrm{K}$), new diffraction lines are observed which are indexed with a crystal unit cell under the condition $h+k+l=2n+1$. These new diffraction lines are related to an antiferromagnetic ordering ($T<T_N$) with a propagation vector $\mathbf{q}=[001]$. A second set of magnetic
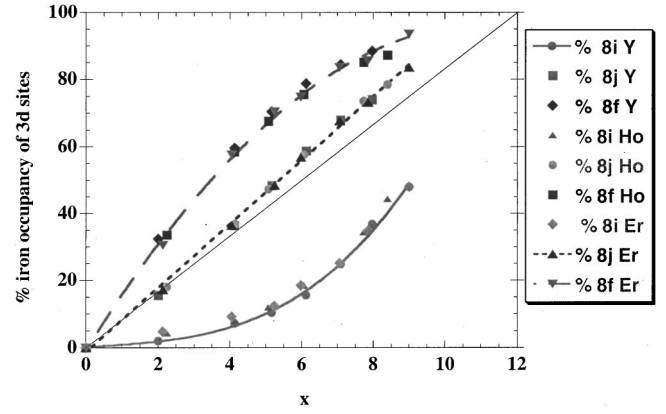
FIG. 2. Iron occupancy scheme of the $3d$ sites in the $R\mathrm{Mn}_{12-x}\mathrm{Fe}_x$ series.

contributions appears on the nuclear peaks at $T=T_C$ ($<T_N$) that is characteristic of a ferromagnetic ordering ($\mathbf{q}'=[000]$) previously observed at low temperatures on the magnetization curves.[5]

The $I4/mmm$ space group is the semidirect product of the point group $P4/mmm$ by the translation I ($\frac{1}{2}$, $\frac{1}{2}$, $\frac{1}{2}$). All possible arrangements of the magnetic moments were deduced from the group theoretical analysis, and the basis vectors were built using the projection operator technique.[9] The ten irreducible representations of the point group $P4/mmm$ are listed in Table I (some errors were detected in a previous analysis[4]). The basis vectors for each magnetic site are listed in Table II, with the atoms numbered according to the space group description in the International Tables for Crystallography (first volume, group $I4/mmm$ No. 139). The average values of the x_{8i} and x_{8j}, position parameters of the $8i$ and

TABLE I. The 10 irreducible representations of the point group $P4/mmm$. $E, 2_z, 4_z, \ldots$ denote the 16 different symmetry operators.

		E	2_z	4_z 4_z^3	2_x 2_y	2_{xy} $2_{\bar{x}y}$	$\bar{1}$	m_{xy}	$\bar{4}_z$ $\bar{4}_z^3$	m_{yz} m_{xz}	$m_{\bar{x}yz}$ m_{xyz}
Γ^1	A_{1g}	1	1	1	1	1	1	1	1	1	1
Γ^2	A_{2g}	1	1	1	-1	-1	1	1	1	-1	-1
Γ^3	B_{1g}	1	1	-1	1	-1	1	1	-1	1	-1
Γ^4	B_{2g}	1	1	-1	-1	1	1	1	-1	-1	1
Γ^5	E_g	$\begin{pmatrix}1&0\\0&1\end{pmatrix}$	$\begin{pmatrix}-1&0\\0&-1\end{pmatrix}$	$\begin{pmatrix}0&1\\-1&0\end{pmatrix}$ $\begin{pmatrix}0&-1\\1&0\end{pmatrix}$	$\begin{pmatrix}1&0\\0&-1\end{pmatrix}$ $\begin{pmatrix}-1&0\\0&1\end{pmatrix}$	$\begin{pmatrix}0&1\\1&0\end{pmatrix}$ $\begin{pmatrix}0&-1\\-1&0\end{pmatrix}$	$\begin{pmatrix}1&0\\0&1\end{pmatrix}$	$\begin{pmatrix}-1&0\\0&-1\end{pmatrix}$	$\begin{pmatrix}0&1\\-1&0\end{pmatrix}$ $\begin{pmatrix}0&-1\\1&0\end{pmatrix}$	$\begin{pmatrix}1&0\\0&-1\end{pmatrix}$ $\begin{pmatrix}-1&0\\0&1\end{pmatrix}$	$\begin{pmatrix}0&1\\1&0\end{pmatrix}$ $\begin{pmatrix}0&-1\\-1&0\end{pmatrix}$
Γ^6	A_{1u}	1	1	1	1	1	-1	-1	-1	-1	-1
Γ^7	A_{2u}	1	1	1	-1	-1	-1	-1	-1	1	1
Γ^8	B_{1u}	1	1	-1	1	-1	-1	-1	1	-1	1
Γ^9	B_{2u}	1	1	-1	-1	1	-1	-1	1	1	-1
Γ^{10}	E_u	$\begin{pmatrix}1&0\\0&1\end{pmatrix}$	$\begin{pmatrix}-1&0\\0&-1\end{pmatrix}$	$\begin{pmatrix}0&1\\-1&0\end{pmatrix}$ $\begin{pmatrix}0&-1\\1&0\end{pmatrix}$	$\begin{pmatrix}1&0\\0&-1\end{pmatrix}$ $\begin{pmatrix}-1&0\\0&1\end{pmatrix}$	$\begin{pmatrix}0&1\\1&0\end{pmatrix}$ $\begin{pmatrix}0&-1\\-1&0\end{pmatrix}$	$\begin{pmatrix}-1&0\\0&-1\end{pmatrix}$	$\begin{pmatrix}1&0\\0&1\end{pmatrix}$	$\begin{pmatrix}0&-1\\1&0\end{pmatrix}$ $\begin{pmatrix}0&1\\-1&0\end{pmatrix}$	$\begin{pmatrix}-1&0\\0&1\end{pmatrix}$ $\begin{pmatrix}1&0\\0&-1\end{pmatrix}$	$\begin{pmatrix}0&-1\\-1&0\end{pmatrix}$ $\begin{pmatrix}0&1\\1&0\end{pmatrix}$

TABLE II. Basis vectors of the irreducible representations for the $8i$, $8j$, $8f$, and $2a$ sites. The F, G, C, and A symbols represent, respectively, the spin (S) configurations $++++$, $+-+-$, $++--$, and $+--+$. The indices 1–4 correspond to the atoms numbered according to International Tables for Crystallography.

		$8i,8j$		$8f$		$2a$	
		x, y	z	x, y	z	x, y	z
Γ^1	A_{1g}			$G_x - A_y$			
Γ^2	A_{2g}		F_z	$A_x + G_y$	F_z		S_z
Γ^3	B_{1g}			$G_x + A_y$	C_z		
Γ^4	B_{2g}		C_z	$A_x - G_y$			
Γ^5	E_g	$\begin{pmatrix} S_{1x}+S_{2x} & S_{3y}+S_{4y} \\ S_{3x}+S_{4x} & S_{1y}+S_{2y} \end{pmatrix}$		$\begin{pmatrix} +F_x & -F_y \\ -C_y & +C_x \end{pmatrix}$	$\begin{pmatrix} +A_z & -G_z \\ -A_z & +G_z \end{pmatrix}$	$\begin{pmatrix} +S_x & -S_y \\ -S_x & +S_y \end{pmatrix}$	
Γ^6	A_{1u}	$S_{1x}-S_{2x}+S_{3y}-S_{4y}$		A_x+G_y	F_z		
Γ^7	A_{2u}	$S_{1y}-S_{2y}-S_{3x}+S_{4x}$		A_y-G_x			
Γ^8	B_{1u}	$S_{1x}-S_{2x}-S_{3y}+S_{4y}$		G_y-A_x			
Γ^9	B_{2u}	$S_{1y}-S_{2y}+S_{3x}-S_{4x}$		G_x+A_y	C_z		
Γ^{10}	E_u		$\begin{pmatrix} S_{3z}-S_{4z} & S_{1z}-S_z \\ S_{3z}-S_{4z} & S_{1z}-S_{2z} \end{pmatrix}$	$\begin{pmatrix} +F_y & +F_x \\ +C_x & +C_y \end{pmatrix}$	$\begin{pmatrix} +G_z & +A_z \\ +G_z & +A_z \end{pmatrix}$		

$8j$ sites, are, respectively, 0.36 and 0.28.[7]

For the $YMn_{12-x}Fe_x$ compounds with $x \le 7$, the best agreement between the calculated and the observed intensities for $T \le T_N$ corresponds to a noncollinear antiferromagnetic structure of $3d(Mn, Fe)$ moments in the basal plane (a, b) belonging to the B_{1u} group representation (Fig. 3). For the YMn_4Fe_8 compound and $T \le T_N < T_C$, the ferromagnetic components on the $3d(8i, 8j, 8f)$ sites along the c axis, belonging to the A_{2g} representation, are superimposed on the previously determined $3d$ antiferromagnetic system.

If R is a magnetic rare earth, the onset of T_C ($<T_N$) for the manganese-rich compounds ($R=Er$, $x<7$; $R=Ho$, $x<6$; $R=Nd$, $x=4,5$) is due to the ferromagnetic component on the rare-earth sites lying along the c axis (A_{2g} representation). The $3d$ antiferromagnetic system previously determined in the $YMn_{12-x}Fe_x$ compounds still remains.

For the iron-rich compounds, strong ferromagnetic [with the light rare earth Nd, $J=L+S$ (Ref. 10)] or ferrimagnetic [with the heavy rare earths Er and Ho, $J=L-S$ (Ref. 10)] couplings occur on the $3d(8j, 8f)$ and $R(2a)$ sites along the c axis. However, the previously described $3d$ antiferro-

FIG. 3. Projection in the basal plane (a, b) of the $3d(Mn, Fe)$ antiferromagnetic structure.

magnetic arrangement on the basal plane (a, b) is still observed.

For the very-iron-rich compound with $x=9$, a purely ferrimagnetic configuration along the c axis, similar to the one observed in the $RFe_{12-y}M_y$ compounds ($y \le 2$, $M=Mo$, Ti, and V), is observed.[3]

The refined magnetic moments at $T=2$ K and the associated ordering temperatures are listed in Table III. They correspond to excellent reliability factors not exceeding 5%.

V. DISCUSSION

A. Structural properties

In a first approach, the substitution scheme of Mn by Fe atoms in the ($8i$, $8j$, $8f$) sites of the $RMn_{12-x}Fe_x$ series has been explained by size effect considerations between these two atoms.[7] The scheme of d-element occupation is experimentally found to be exactly the same, independent of the choice of the rare-earth element R, i.e., of the size of R. For all R, iron atoms are located preferentially on the $8f$ sites which present the smallest volume of Voronoi polyhedra, whereas manganese atoms with a larger radius occupy the $8i$ sites, having the biggest volume of Voronoi polyhedra. Indeed, the relatively poor affinity of iron atoms found experimentally for the $8i$ site is consistent with the impossibility of stabilizing the RFe_{12} compounds and with the existence of the isotypes RM_{12}.[3] This also supports the local structure arguments based on the enthalpy of formation of binary R_xT_y compounds (here $T=Mn$ or Fe).[1]

For a given iron content, the a and c cell parameters decrease when Z_R, the atomic number of the R elements, increases and follow the lanthanides contraction.[3] In addition, the substitution of manganese (12.8 Å^3) by iron, with a smaller atomic volume (11.77 Å^3), leads to a linear decrease of the a cell parameter, whereas the c cell parameter is found to be slightly modified as a function of x. These different
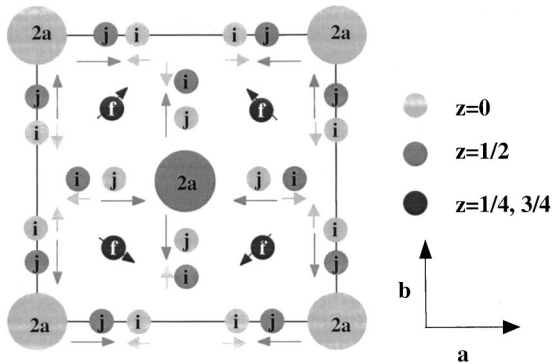
TABLE III. Amplitude (μ_B/f.u.) and deviation θ (degrees) from the **c** axis of the magnetic moments and ordering temperatures T_C and T_N (K) of the RMn$_{12-x}$Fe$_x$ series with $R=$Nd, Er, Ho, and Y. Numbers in parentheses represent errors on the last digit for the magnetic moment values; the errors made on the determination of the ordering temperatures are estimated at 10 K. The magnetic moments of the HoMn$_{12}$ and HoMn$_3$Fe$_9$ compounds have not been refined due to the important presence of, respectively, Ho$_6$Mn$_{23}$ and Ho$_2$Fe$_{17}$ ferromagnetic impurities.

		NdMn$_{12-x}$Fe$_x$	HoMn$_{12-x}$Fe$_x$	ErMn$_{12-x}$Fe$_x$	YMn$_{12-x}$Fe$_x$
$x=0$	$\mu 8i$			−0.76 (1)	−0.76 (1)
	$\theta 8i$			90°	90°
	$\mu 8j$			0.38 (1)	0.77 (3)
	$\theta 8j$			90°	90°
	$\mu 8f$			0.47 (1)	0.24 (2)
	$\theta 8f$			90°	90°
	$\mu 2a$			6.0 (4)	
	$\theta 2a$			0°	
	T_C			4 K	
	T_N			80 K	134 K
$x=2$	$\mu 8i$		−1.04 (2)	−0.81 (2)	−0.90 (8)
	$\theta 8i$		90°	90°	90°
	$\mu 8j$		0.56 (1)	0.60 (2)	0.86 (7)
	$\theta 8j$		90°	90°	90°
	$\mu 8f$		0.30 (1)	0.2 (2)	0.14 (6)
	$\theta 8f$		90°	90°	90°
	$\mu 2a$		0	2.5 (3)	
	$\theta 2a$		0°	0°	
	T_C		<2 K	4 K	
	T_N		170 K	175 K	190 K
$x=3$	$\mu 8i$		−1.29 (2)	−1.06 (2)	
	$\theta 8i$		90°	90°	
	$\mu 8j$		0.89 (2)	0.79 (2)	
	$\theta 8j$		90°	90°	
	$\mu 8f$		0.26 (1)	0.4 (1)	
	$\theta 8f$		90°	90°	
	$\mu 2a$		3.3 (4)	0	
	$\theta 2a$		0°	0°	
	T_C		<2 K	<2 K	
	T_N		205 K	210 K	
$x=4$	$\mu 8i$	−1.65 (5)	−1.41 (4)	−1.2 (1)	−1.4 (1)
	$\theta 8i$	90°	90°	90°	90°
	$\mu 8j$	1.39 (4)	1.17 (3)	1.09 (8)	1.41 (9)
	$\theta 8j$	90°	90°	90°	90°
	$\mu 8f$	0.87 (6)	0.44 (6)	0.006 (70)	0.3 (1)
	$\theta 8f$	90°	90°	90°	90°
	$\mu 2a$	0	4.6 (3)	0	
	$\theta 2a$	0°	0°	0°	
	T_C	<2 K	10 K	<2 K	
	T_N	230 K	230 K	230 K	230 K
$x=5$	$\mu 8i$	−1.6 (1)	−1.3 (1)	−1.36 (3)	−1.5 (1)
	$\theta 8i$	90°	90°	90°	90°
	$\mu 8j$	1.34 (8)	1.37 (6)	1.27 (3)	1.4 (1)
	$\theta 8j$	90°	90°	90°	90°
	$\mu 8f$	0.78 (8)	0.56 (7)	0.70 (3)	0.4 (1)
	$\theta 8f$	90°	90°	90°	90°
	$\mu 2a$	0.9 (3)	5.9 (2)	6.8 (6)	
	$\theta 2a$	0°	0°	0°	

TABLE III. (*Continued.*)

		$\mathrm{NdMn}_{12-x}\mathrm{Fe}_x$	$\mathrm{HoMn}_{12-x}\mathrm{Fe}_x$	$\mathrm{ErMn}_{12-x}\mathrm{Fe}_x$	$\mathrm{YMn}_{12-x}\mathrm{Fe}_x$
	T_C	11 K	20 K	8 K	
	T_N	240 K	230 K	235 K	240 K
$x=6$	$\mu 8i$	−1.36 (9)	−1.17 (6)	−1.07 (3)	−1.36 (6)
	$\theta 8i$	90°	90°	90°	90°
	$\mu 8j$	1.04 (8)	1.4 (1)	1.32 (5)	1.29 (5)
	$\theta 8j$	90°	69.4°	90°	90°
	$\mu 8f$	0.9 (1)	0.95 (6)	0.7 (1)	0.74 (6)
	$\theta 8f$	76°	69.1°	90°	90°
	$\mu 2a$	1.7 (1)	6.4 (2)	6.0 (3)	
	$\theta 2a$	0°	0°	0°	
	T_C	<80 K	80 K	14 K	
	T_N	230 K	230 K	230 K	230 K
$x=7$	$\mu 8i$		−1.07 (9)	−0.90 (2)	−1.33 (3)
	$\theta 8i$		90°	90°	90°
	$\mu 8j$		1.23 (9)	1.28 (7)	1.12 (3)
	$\theta 8j$		51.6°	68.9°	90°
	$\mu 8f$		1.09 (8)	0.98 (5)	0.77 (3)
	$\theta 8f$		33°	61.9°	90°
	$\mu 2a$		8.7 (1)	6.4 (1)	
	$\theta 2a$		0°	0°	
	T_C		185 K	100 K	
	T_N		210 K	210 K	197 K
$x=8$	$\mu 8i$		−0.77 (9)	−0.8 (1)	1.3 (2)
	$\theta 8i$		84.8°	90°	67.4°
	$\mu 8j$		1.20 (7)	1.1 (1)	1.2 (2)
	$\theta 8j$		34.1°	26.86°	17.7°
	$\mu 8f$		1.01 (3)	0.97 (5)	1.0 (2)
	$\theta 8f$		0°	0°	11.2°
	$\mu 2a$		8.92 (6)	7.1 (1)	
	$\theta 2a$		0°	0°	
	T_C		260 K	203 K	250 K
	T_N		168 K	160 K	150 K
$x=9$	$\mu 8i$			−0.38 (7)	
	$\theta 8i$			0°	
	$\mu 8j$			−1.61 (8)	
	$\theta 8j$			0°	
	$\mu 8f$			−1.50 (6)	
	$\theta 8f$			0°	
	$\mu 2a$			7.7 (1)	
	$\theta 2a$			0°	
	T_C			320 K	

.

observations mean that there is a direct control of the cell parameters in terms of R-(Mn, Fe) and (Mn, Fe)-(Mn, Fe) bonds for a and R-(Mn, Fe) only for c. In fact, for the latter parameter, the $3d$-substitution schemes on the $8f$ and $8j$ sites seem to approximately compensate in terms of bond length. Finally, one observes that the slope of the decreasing cell volume is fairly independent of the rare-earth element.

B. Magnetic properties

For the manganese-rich compounds ($x<6$), the AF magnetic structure of YMn_{12} type, as shown in Fig. 3, is the reference magnetic arrangement for the $3d$(Mn, Fe) sublattices. An indirect ferromagnetic interaction acts between the rare-earth sites (in the $2a$ positions 0, 0, 0 and $\frac{1}{2}$, $\frac{1}{2}$, $\frac{1}{2}$) through the $8f(3d)$ moments (in the $8f$ positions $\frac{1}{4}$, $\frac{1}{4}$, $\frac{1}{4}$). The corresponding critical ordering temperature T_C remains very low (typically <20 K) for all rare-earth elements.

However, the stronger AF couplings acting between most of the $3d$ sites are progressively superseded by ferromagnetic ones supported by the substitution scheme of iron for manganese, first and dominantly on the $8f$ and $8j$ sites. Similarly to the change of type of exchange forces, the $3d$
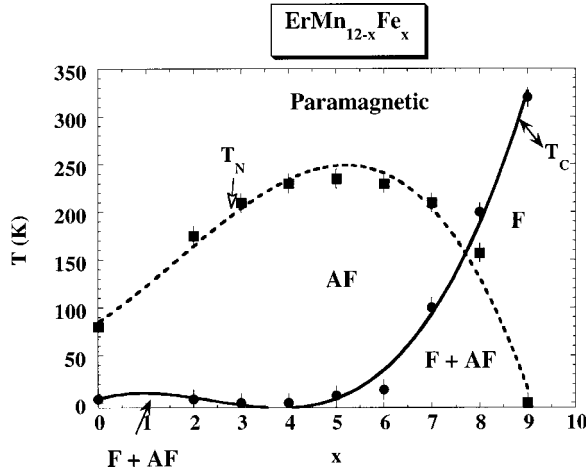
FIG. 4. Magnetic phase diagram of the $ErMn_{12-x}Fe_x$ compounds. The notation F and AF corresponds, respectively, to ferromagnetic and antiferromagnetic behaviors.

magnetocrystalline anisotropy transforms from a planar[4] to an axial character.[3] The corresponding magnetic phase diagram of the Er compounds is represented in Fig. 4. The same type of phase diagram is obtained for $R=$ Ho and Nd. Nevertheless, shifts of the various magnetic phases towards lower iron contents are observed. This last feature can be related to the larger size of these rare-earth elements.

Since the $3d$ occupation scheme does not depend on the nature of the rare-earth element, it is noteworthy that for $x<6$ the dependence of T_N on x mimics those of the $8i$ and $8j$ magnetic moments quite well as revealed in Fig. 5. A small additional dependence on the $4d(Y)$ or $5d(R)$ orbitals for $x\leq3$ is observed. For $x<6$, the $8i$ and $8j$ magnetic moments verify the relationship $\mu_{3d}(R=\text{Er})\leq\mu_{3d}(R=\text{Ho})\leq\mu_{3d}(R=\text{Y})\leq\mu_{3d}(R=\text{Nd})$, which can be related to the corresponding cell volumes (i.e., local atomic volume) $V(\text{Er})<V(\text{Ho})<V(\text{Y})<V(\text{Nd})$, a larger volume favoring stronger moments on the $8i$ and $8j$ sites.[11]

The magnitudes of the $8f$ and $2a$ (Fig. 6) magnetic moments vary in quite similar ways over the entire range of compositions. We thus consider that the low ferromagnetic coupling R-R for $x<6$ is of biquadratic exchange type, via the $8f$ sites as previously observed in the isotype compound UFe_4Al_8.[12] In that compound, one is dealing with different components of moments $M_z(R)$-$M_{x,y}(8f)$-$M_z(R)$, with the $4f$ moment directed along the c axis and the $8f$ ones lying in the basal plane (a, b). Due to the competition between opposite interactions in the intermediate range of compositions $(2\leq x\leq4)$, the ferromagnetic exchange coupling via the $4f$-$3d(8f)$-$4f$ path is strongly disturbed. Indeed, the observed ferromagnetism is very weak (Table III) and the exchange coupling is insufficient to establish a long-range ordering as indicated by the large neutron diffuse scattering observed on the basis of the nuclear reflections $(T<10\,\text{K},$ Fig. 7). Evidence of such a phenomenon (ferromagnetic short-range ordering) is found for x compositions for which the $8f$ site is almost statistically occupied by about 50% Fe–50% Mn.
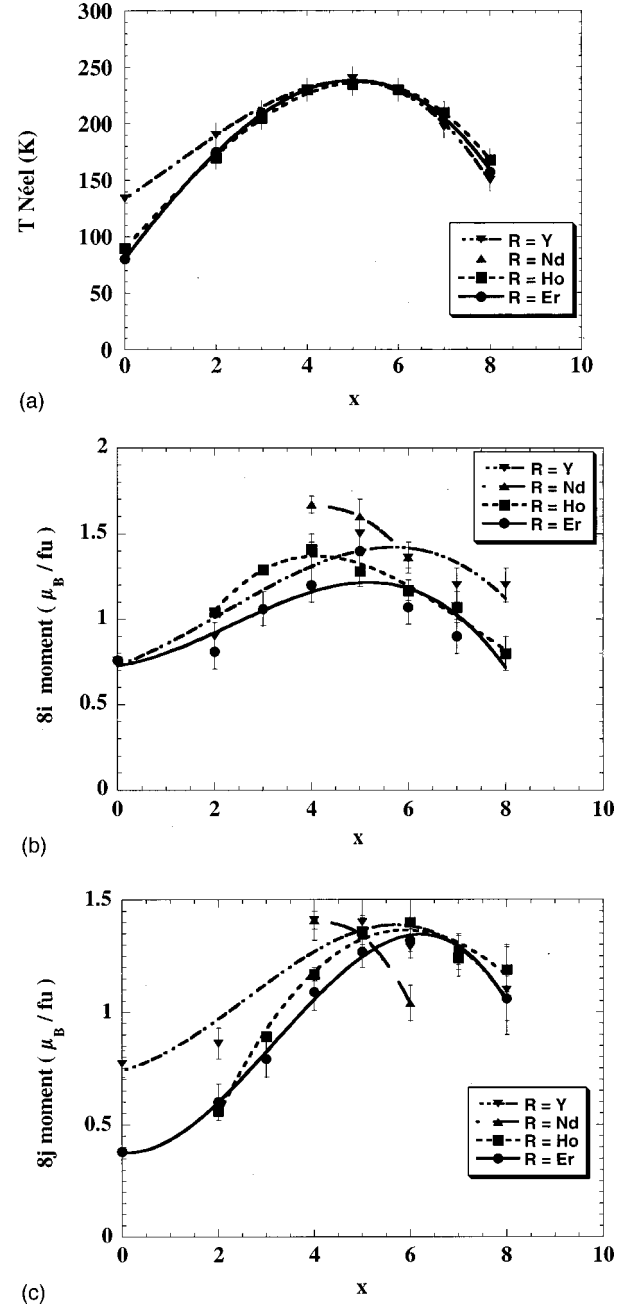
FIG. 5. Behaviors (a) of the Néel temperature and (b) of the $8i(\text{Mn}, \text{Fe})$ and (c) $8j(\text{Mn}, \text{Fe})$ magnetic moments, determined at $T=2\,\text{K}$, in the $RMn_{12-x}Fe_x$ series with $R=$ Y, Ho, Er, and Nd.

For $x\geq6$, the $8f$ and $8j$ sites are dominantly occupied by iron, and then significantly stronger ferromagnetic coupling forces occur. This fact favors stronger and stronger R-$3d$ ferromagnetic $(R=\text{Nd})$ or ferrimagnetic $(R=\text{Ho}$ and Er) couplings in both cases via negative $3d$-$5d$ exchange interactions. Hence, as parallel polarized, the rare-earth magnetic moment increases towards its theoretical saturation value, and the common Curie temperature (from R and $3d$ contributions) increases quite rapidly with x. By contrast, the AF couplings mainly based on the remaining manganese atoms (mainly located in the $8i$ sites) drop progressively and vanish for $x=9$. For $ErMn_3Fe_9$ (Table III), the low values of the $8i$
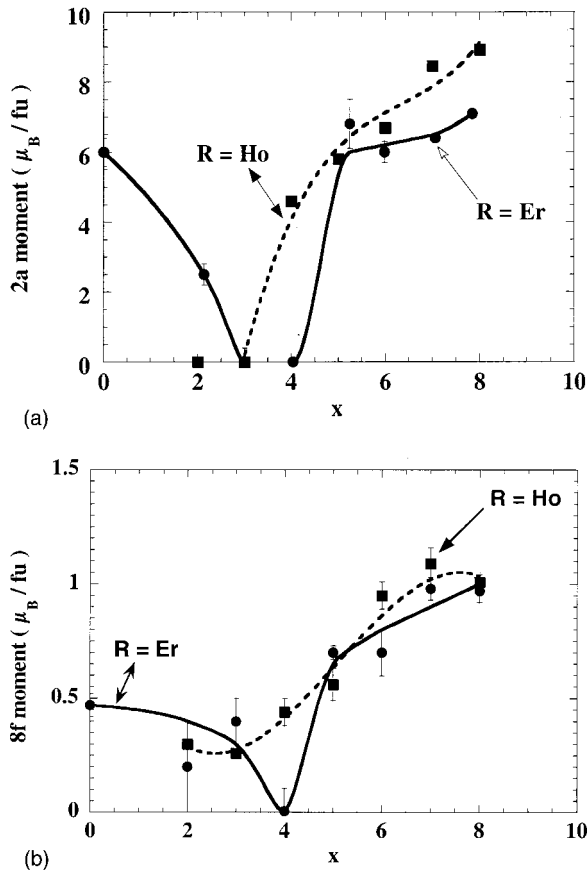
FIG. 6. Behaviors of (a) the $8f$(Mn, Fe) and (b) $2a(R)$ magnetic moments at $T=2$ K in the RMn$_{12-x}$Fe$_x$ series with $R=$ Er and Ho.

ferromagnetic moments (sites occupied by 54% of manganese) compared to the other $8j$ and $8f$ (sites populated in majority by iron) is explained by x-ray magnetic circular dichroism (XMCD) measurements.[13] Indeed, the Mn-Fe negative exchange couplings concern mainly the $8i$ sites.

Crystal electrical field (CEF) effects can explain the easy magnetization direction observed for the rare-earth magnetic moments. Indeed, the anisotropy of the R sublattices arises from the CEF and depends mainly on the sign of the second order term $\alpha_J A_0^2$. In these compounds, the parameter A_0^2 is negative[1,3] and favors an easy magnetic direction along the c

axis for a positive α_J second-order Stevens factor ($R=$Er). For negative α_J ($R=$Ho and Nd), the moment $M(R)$ would lie in the basal plane (a, b). But for $R=$Ho and Nd, α_J is weak[1] and the easy magnetization direction found along the c axis can be explained by introducing higher-order terms (e.g., sixth order), which are not negligible, as it has been found for $R=$Ho (Ref. 3) in the isotype compounds RFe$_{10.5}$Mo$_{1.5}$.

VI. CONCLUSION

The magnetic properties of the RMn$_{12-x}$Fe$_x$ compounds are markedly dependent on both the nature of the $3d$ elements and the scheme of the selective occupation of these elements on the $8f$, $8j$, and $8i$ sublattices. The magnetic arrangements of the $3d$ sublattices are antiferromagnetic for $x<6$. They transform progressively to more complex configurations "F+AF" for $6<x<9$ and, finally, to a purely ferromagnetic one for the iron-rich compounds ($x=9$).

For the iron-rich compounds, it appears that the most important $3d$ ferromagnetic contribution is due to the $8f$ and $8j$ sites. The main location of the manganese remains on the $8i$ site with a local ferromagnetic polarization opposite to the iron one's as deduced from XMCD experiments.[13] In fact, a clustering of local dumbbells is suspected to occur, thus allowing such inverse magnetic moment polarization.

For the manganese-rich compounds, due to the easy plane configuration of the $8f$ sites (AF) and via a biquadratic indirect scheme of coupling, the rare-earth moments order ferromagnetically along the c axis. This corresponds to uncoupled $3d$ and R magnetic sublattices with particularly low Curie temperatures.

In an intermediate range of compositions, competing exchange interactions on the $3d$ sites lead to a decrease or cancellation of any long-range magnetic ordering, mainly concerning the R and $8f$ sites.

Further work is in progress on these magnetic systems by using both neutron diffraction experiments and magnetization measurements.[5] This includes measurements in progress using resistivity, magnetoresistivity, x-ray spectroscopy at the $K(3d)$, $L_{II,III}(3d,R)$, and $M_{IV,V}(R)$ edges (in particular for $x=8$), and electronic structure calculations.
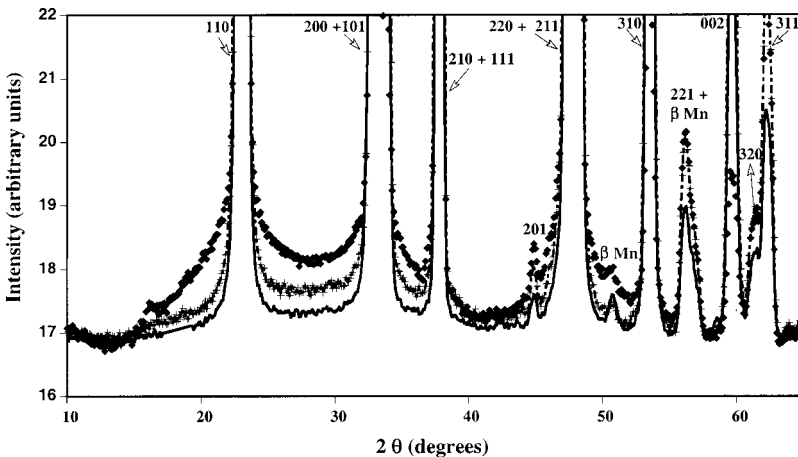
FIG. 7. Neutron diffraction patterns at $T=2$ K ($\blacklozenge$), $T=4$ K ($\times$), and $T=6$ K (solid line) of the ErMn$_7$Fe$_5$ compound showing the marked diffuse scattering related to a ferromagnetic short-range ordering.

*Corresponding author. FAX: 33-(0)4-76-88-10-38. Electronic address: morales@polycnrs-gre.fr

[1] K. H. J. Buschow and D. B. de Mooij, in *Concerted European Action on Magnets (CEAM)*, edited by I. V. Mitchell *et al.* (Elsevier, New York, 1989), p. 53.

[2] J. V. Florio, R. E. Rundle, and A. I. Snow, Acta Crystallogr. **5**, 449 (1952).

[3] E. Tomey, Ph.D. thesis, Université J. Fourier, Grenoble, France, 1994.

[4] J. Deportes and D. Givord, Solid State Commun. **19**, 845 (1976).

[5] M. Morales, M. Bacmann, D. Fruchart, and P. Wolfers, J. Magn. Magn. Mater. **196**, 703 (1999).

[6] J. Rodriguez-Carvajal, Physica B **192**, 55 (1993).

[7] M. Artigas, M. Bacmann, D. Fruchart, M. Morales, and E. Tomey, Physica B **234−236**, 155 (1997).

[8] P. Wolfers, J. Appl. Crystallogr. **23**, 554 (1990).

[9] E. F. Bertaut, Acta Crystallogr., Sect. A: Cryst. Phys., Diffr., Theor. Gen. Crystallogr. **24**, 217 (1968).

[10] J. A. Campbell, J. Phys. F: **2**, L47 (1972).

[11] O. Isnard and D. Fruchart, J. Alloys Compd. **205**, 1 (1994).

[12] J. Paixao *et al.*, Phys. Rev. B **55**, 14 370 (1997).

[13] M. Morales, M. Bacmann, D. Fruchart, P. Wolfers, Ch. Baudelet, A. Delobbe, and G. Krill, J. Alloys Compd. **317**, 470 (2001).